Gynecologic Oncology 167 (2022) 96–106

Contents lists available at ScienceDirect

Gynecologic Oncology

journal homepage: www.elsevier.com/locate/ygyno

A novel cell line panel reveals non-genetic mediators of platinum resistance and phenotypic diversity in high grade serous ovarian cancer

J.I. Hoare [a,1], H. Hockings [a,1], J. Saxena [a], V.L. Silva [a], M.J. Haughey [b], G.E. Wood [c], F. Nicolini [a], H. Mirza [d], I.A. McNeish [d], W. Huang [b], E. Maniati [e], T.A. Graham [f], M. Lockley [f,g,*]

[a] Centre for Cancer Cell and Molecular Biology, Barts Cancer Institute, Queen Mary University of London, London, UK
[b] School of Mathematical Sciences, Queen Mary University of London, London, UK
[c] Centre for Tumour Biology, Barts Cancer Institute, Queen Mary University of London, London, UK
[d] Department of Surgery and Cancer, Imperial College London, London, UK
[e] Bioinformatics Core Service, Barts Cancer Institute, Queen Mary University of London, London, UK
[f] Centre for Cancer Genomics and Computational Biology, Barts Cancer Institute, Queen Mary University of London, London, UK
[g] Department of Gynaecological Oncology, Cancer Services, University College London Hospital, London, London, UK

HIGHLIGHTS

- A new panel of platinum-resistant HGSC cell lines and *in vivo* models that are easy to use in standard laboratory conditions.
- Resistant HGSC cell lines evolved from a pre-existing clone without a unifying mutational cause for drug resistance.
- Recurrent changes in gene expression were shared by resistant HGSC cells and multiple patients with resistant HGSC.
- Extracellular matrix-related genes and pathways were repeatedly expressed by resistant HGSC cell lines and human patients.
- Resistant HGSC cell lines produced diverse intraperitoneal behaviours that reflect relapsed human HGSC.

ARTICLE INFO

Article history:
Received 28 April 2022
Received in revised form 18 July 2022
Accepted 23 July 2022
Available online 30 July 2022

Keywords:
High grade serous ovarian cancer
Drug resistance
Platinum
Chemotherapy
Evolution
Transcription
Gene expression
Non-genetic
Extracellular matrix

ABSTRACT

Objectives. Resistance to cancer therapy is an enduring challenge and accurate and reliable preclinical models are lacking. We interrogated this unmet need using high grade serous ovarian cancer (HGSC) as a disease model.

Methods. We created five *in vitro* and two *in vivo* platinum-resistant HGSC models and characterised the entire cell panel *via* whole genome sequencing, RNASeq and creation of intraperitoneal models.

Results. Mutational signature analysis indicated that platinum-resistant cell lines evolved from a pre-existing ancestral clone but a unifying mutational cause for drug resistance was not identified. However, cisplatin-resistant and carboplatin-resistant cells evolved recurrent changes in gene expression that significantly overlapped with independent samples obtained from multiple patients with relapsed HGSC. Gene Ontology Biological Pathways (GOBP) related to the tumour microenvironment, particularly the extracellular matrix, were repeatedly enriched in cisplatin-resistant cells, carboplatin-resistant cells and also in human resistant/refractory samples. The majority of significantly over-represented GOBP however, evolved uniquely in either cisplatin- or carboplatin-resistant cell lines resulting in diverse intraperitoneal behaviours that reflect different clinical manifestations of relapsed human HGSC.

Conclusions. Our clinically relevant and usable models reveal a key role for non-genetic factors in the evolution of chemotherapy resistance. Biological pathways relevant to the extracellular matrix were repeatedly expressed by resistant cancer cells in multiple settings. This suggests that recurrent gene expression changes provide a fitness advantage during platinum therapy and also that cancer cell-intrinsic mechanisms influence the tumour microenvironment during the evolution of drug resistance. Candidate genes and pathways identified here could reveal therapeutic opportunities in platinum-resistant HGSC.

* Corresponding author at: Reader in Medical Oncology, Centre for Cancer Genomics and Computational Biology, Barts Cancer Institute, Queen Mary University of London, John Vane Science Centre, Charterhouse Square, London EC1M 6BQ, UK.
E-mail address: m.lockley@qmul.ac.uk (M. Lockley).
[1] These authors contributed equally.

https://doi.org/10.1016/j.ygyno.2022.07.027

1. Introduction

High Grade Serous Carcinoma (HGSC), the most common ovarian cancer subtype [1], is treated with surgery and platinum-based chemotherapy but approximately 80% of patients relapse and respond less well to successive platinum-containing chemotherapy regimens [2,3]. Most women relapse with widespread metastasis and recurrent ascites [4], but some experience oligo-metastatic recurrence, usually with a more indolent disease course [5]. Platinum-resistance is defined clinically when relapse occurs within 6 months of the most recent platinum treatment [6]. Effective therapeutic options in this situation are extremely limited and median overall survival is approximately 12 months [7,8]. Maintenance treatment with PARP inhibitors dramatically improves progression-free survival in platinum-sensitive disease [9–14] but new treatments, including PARP inhibitors, have failed to improve survival in platinum-resistant HGSC. Diverse molecular features of platinum-resistant HGSC have been described [2,15,16] but how these direct clinical behaviour is still largely unknown.

There are no widely accepted laboratory models of platinum-resistant HGSC to interrogate this clinical challenge. This is likely because the routine *ex vivo* culture of HGSC and creation of permanent cell lines is extremely challenging and has only rarely been achieved [17,18]. Research therefore relies heavily on commercially available cell lines. Domcke *et al* [19] compared the genomes of 47 ovarian cancer cell lines to the TCGA dataset and demonstrated that several of the most commonly used cells, *e.g.* A2780 and SKOV3, represent human HGSC poorly. Thus although cisplatin and paclitaxel resistant versions of A2780 and SKOV3 (A2780cp and SKOV3-TR [20]) are widely utilised, their relevance for human resistant HGSC is questionable. Domcke *et al* defined several cell lines as "likely high grade serous" including OVCAR4, Cov318 and Ovsaho and subsequent work has demonstrated their utility for laboratory research [21,22]. We use these three cell lines to create a novel panel of platinum-resistant *in vitro* and *in vivo* HGSC models and present an extensive characterisation of these new laboratory tools. We show that they recapitulate the transcriptomic and clinical features of relapsed human HGSC and demonstrate their potential to reveal new insights into platinum-resistant HGSC.

2. Results

2.1. Platinum-resistance can be induced in HGSC cell lines and maintained after drug withdrawal

Cisplatin- and carboplatin-resistant HGSC cells were derived from OVCAR4, Ovsaho and Cov318, which have been categorised as "likely high grade serous" [19]. Cells were cultured *in vitro* in either cisplatin or carboplatin dosed either at IC_{50} or with gradually increasing drug concentrations. Resistant cell lines were only generated successfully using increasing doses. Dose escalation stopped once a 2–10 fold increase in IC_{50} was achieved to reflect the resistance observed in human patients [23]. Cells were immediately bulked and stored and low passage cells were used in all subsequent experiments. Cisplatin-resistant (Ov4Cis, OvsahoCis, CovCis) and carboplatin-resistant (Ov4Carbo and OvsahoCarbo) cell lines were then either cultured at the same drug dose (Ov4Cis: 0.6 μM, OvsahoCis: 0.7 μM, CovCis: 0.7 μM, Ov4Carbo 3.5 μM, OvsahoCarbo 5 μM) or without drug (denoted ND) for eight weeks and IC_{50} was measured again to determine if resistance was maintained in the absence of drug (Fig. 1). Significant resistance to carboplatin was not achieved in Cov318 cells (Fig. 1C) but in all other cases, resistance was induced successfully. In OVCAR4-derived cells (Ov4Cis and Ov4Carbo), resistance to cisplatin and carboplatin was stable following drug withdrawal (Fig. 1A). OvsahoCis cells also maintained resistance when drug was withdrawn (Fig. 1B) but in OvsahoCarbo (Fig. 1B) and CovCis (Fig. 1C), resistance diminished over time after removal of drug from the culture medium ($P < 0.05$).

2.2. Platinum resistance is comparable whether it is induced by cisplatin or carboplatin, in vitro or in vivo

OVCAR4-derived cells were transfected with lentiviruses expressing Firefly luciferase (Luc) to facilitate *in vivo* generation of drug resistant tumours. Resulting cell lines were denoted OVCAR4-Luc, Ov4Cis-Luc and Ov4Carbo-Luc. *In vitro* resistance to cisplatin (Fig. 2A) and carboplatin (Fig. 2B) was maintained in these transfected cells. Interestingly, all cell lines were cross-resistant to cisplatin and carboplatin regardless of the platinum compound initially used to induce resistance (Fig. 2A-B).

We next induced platinum resistance in a more clinically representative intraperitoneal (IP) *in vivo* model. Female nude mice were injected IP with either OVCAR4-Luc (Fig. 2C) or Ov4Carbo-Luc cells (Fig. 2D). Once tumours had established (day 22), mice were treated weekly with either 50 mg/kg carboplatin or vehicle IP for four weeks. Tumour growth was monitored with bioluminescence imaging (BLI). As expected, Ov4Carbo-Luc cells were resistant to carboplatin and light emission overlapped with vehicle-treated control mice (Fig. 2D). In contrast, mice with OVCAR4-Luc IP xenografts initially responded to carboplatin but tumours eventually regrew indicating *in vivo* development of carboplatin-resistance (Fig. 2C). The IP OVCAR4-Luc tumours of two carboplatin-treated mice were harvested at end point, (Fig. 2E) and resulting cell lines were denoted IVR01 and IVR02 (*In Vivo* Resistant 1 and 2). IVR01 and IVR02 were harvested 12 weeks after the last platinum treatment, indicating that resistance was stable after drug withdrawal in these cell lines. *In vitro* (Ov4Carbo) and *in vivo* (IVR01 and IVR02) derived carboplatin-resistant cells had equivalent IC_{50} to carboplatin (all $P < 0.0001$ compared to OVCAR4) (Fig. 2F), despite the different contexts (*in vitro vs. in vivo*), drug doses and scheduling of treatments. This overlap provided reassurance regarding the relevance of our *in vitro*-derived models to platinum resistance induced within the IP environment of HGSC.

2.3. Whole genome sequencing of cisplatin-resistant HGSC cells indicates evolution from a pre-existing ancestral clone

We investigated routes to resistance using deep whole genome sequencing of OVCAR4, Ov4Cis and four separate clones grown from individual, cisplatin-resistant Ov4Cis cells (clones 1, 2, 3 and 4) (Fig. 3A). Variant point mutations were identified by comparing to the human reference genome (hg19) and used to construct a phylogenetic tree (Fig. 3B).

In keeping with existing literature [2,15,16], we did not identify mutations that could provide a unifying explanation for platinum resistance. Only two nonsynonymous exonic mutations were shared between all five resistant cells; *FCGBP* (Fc Fragment Of IgG Binding Protein) and *RTL1* (Retrotransposon Gag Like 1). Cisplatin-resistant clones diverged into two main lineages, which appeared to evolve independently. Although these branches were associated with a greater number of mutations, only 161 nonsynonymous mutations separated Ov4Cis from OVCAR4. Mutational signature analysis revealed that COSMIC signatures SBS31; https://cancer.sanger.ac.uk/signatures/sbs/sbs31/ and SBS35; https://cancer.sanger.ac.uk/signatures/sbs/sbs35/, which are both associated with platinum drug treatment, were common to both lineages at high prevalence (Fig. 3C). Both signatures were also found in the trunk of the phylogenetic tree but at low prevalence, suggesting that a rare pre-existing clone was selected during cisplatin treatment and subsequently diverged into the two main lineages.

2.4. Platinum-resistant OVCAR4-derived clones share multiple transcriptional features with platinum resistant/refractory human HGSC

We used RNAseq to assess whether our resistant OVCAR4-derived cell lines (Ov4Cis and Ov4Carbo) shared features with resistant human HGSC. Gene expression differences between Ov4Carbo and platinum-sensitive OVCAR4 cells, as well as gene expression differences

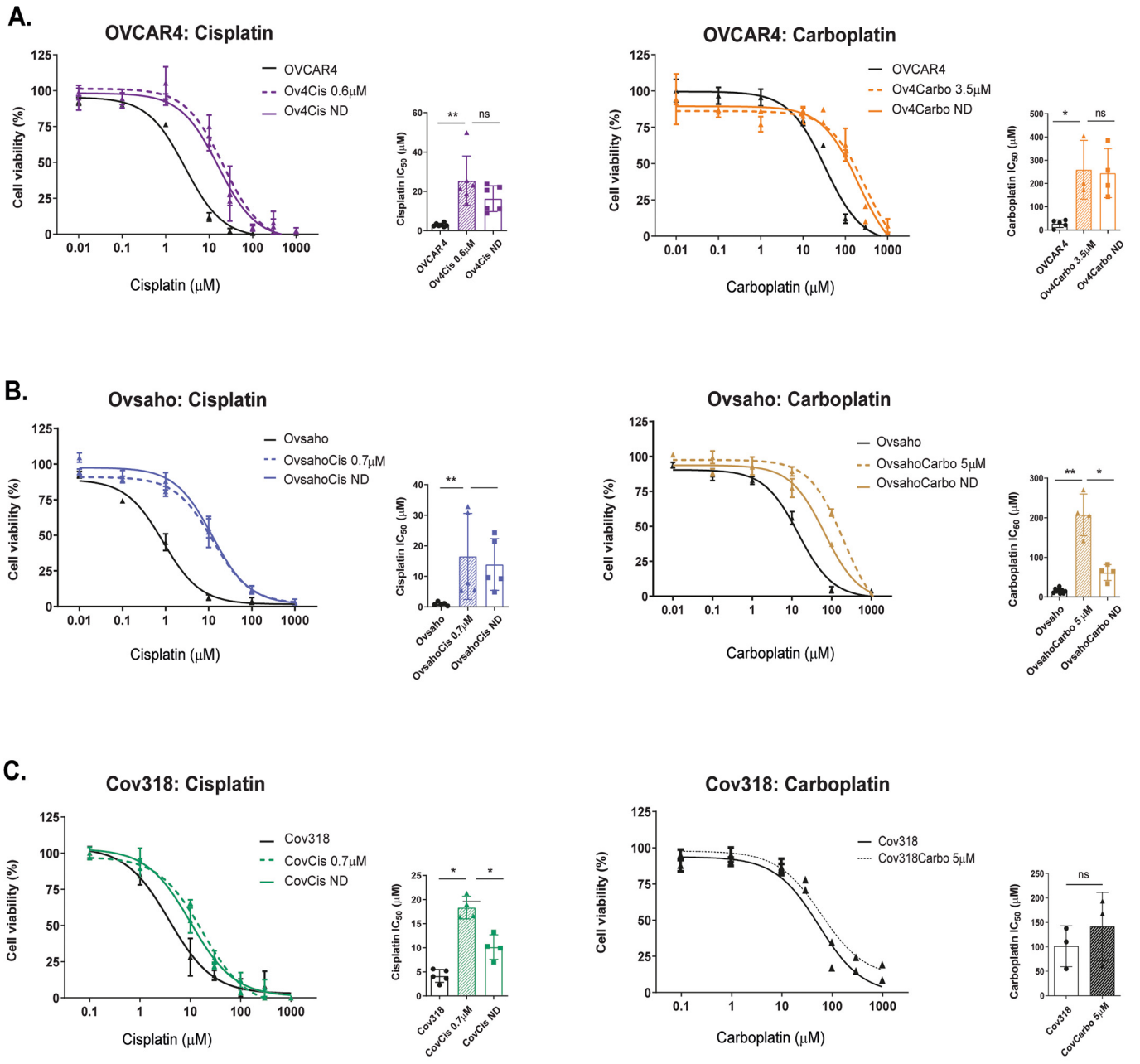

Fig. 1. Platinum-resistance can be induced in HGSC cell lines and is maintained after drug withdrawal.
A. OVCAR4, B. Ovsaho and C. Cov318 cells were cultured in escalating doses of cisplatin or carboplatin. The resulting resistant cell lines (cisplatin-resistant: Ov4Cis (purple), OvsahoCis (blue), CovCis (green) and carboplatin-resistant: Ov4Carbo (orange), OvsahoCarbo (brown), CovCarbo (black)) were then either cultured in the same drug dose (Ov4Cis: 0.6 μm, OvsahoCis: 0.7 μM, CovCis: 0.7 μM, Ov4Carbo 3.5 μM, OvsahoCarbo 5 μM, CovCarbo 5 μM) or without drug (denoted ND) for eight weeks. Dose response and IC_{50} by MTT following 72 h drug treatment is shown. $N = 3$–6, mean ± s.d., unpaired *t*-test, ns = non-significant, $^{*}P < 0.05$, $^{**}P < 0.01$.

between Ov4Cis and OVCAR4 were identified. The ICGC publicly available gene expression database was then interrogated to identify differences between whole tumour tissue obtained from patients with platinum-resistant and refractory HGSC ($n = 49$) compared to patients with platinum-sensitive HGSC ($n = 31$) [25]. Finally, those genes that were differentially expressed between human resistant/refractory and sensitive samples (nominal $P < 0.05$) were compared to the differentially expressed genes that we observed between Ov4Carbo and OVCAR4 and also between Ov4Cis and OVCAR4 (adjusted $P < 0.05$). We observed approximately 330 genes in Ov4Carbo (Fig. 4A, Supplementary Table 1) and 500 genes in Ov4Cis (Fig. 4B, Supplementary Table 1) that had a concordant change with human samples, demonstrating that transcriptional alterations induced by platinum-resistance in our models are also found in platinum-resistant human HGSC. We then compared our resistant cell lines to two other datasets of post-chemotherapy HGSC patient samples. The first identified upregulated adipocyte signatures and stem-like genes [26] and we also found common stem-like genes including *ALDH1A1, ALDH2* and *ALDH1L1* in both Ov4Cis and Ov4Carbo compared to OVCAR4 cells. A second series showed upregulation of AP-1 family genes (*e.g. Fos, Jun* and *TGFβ*) in resistant HGSC [16] and the same three genes were also present in Ov4Cis compared to OVCAR4 cells. Together, these comparisons with three independent sets of post-treatment human samples underpin the utility of our cell line panel for modelling resistant HGSC.

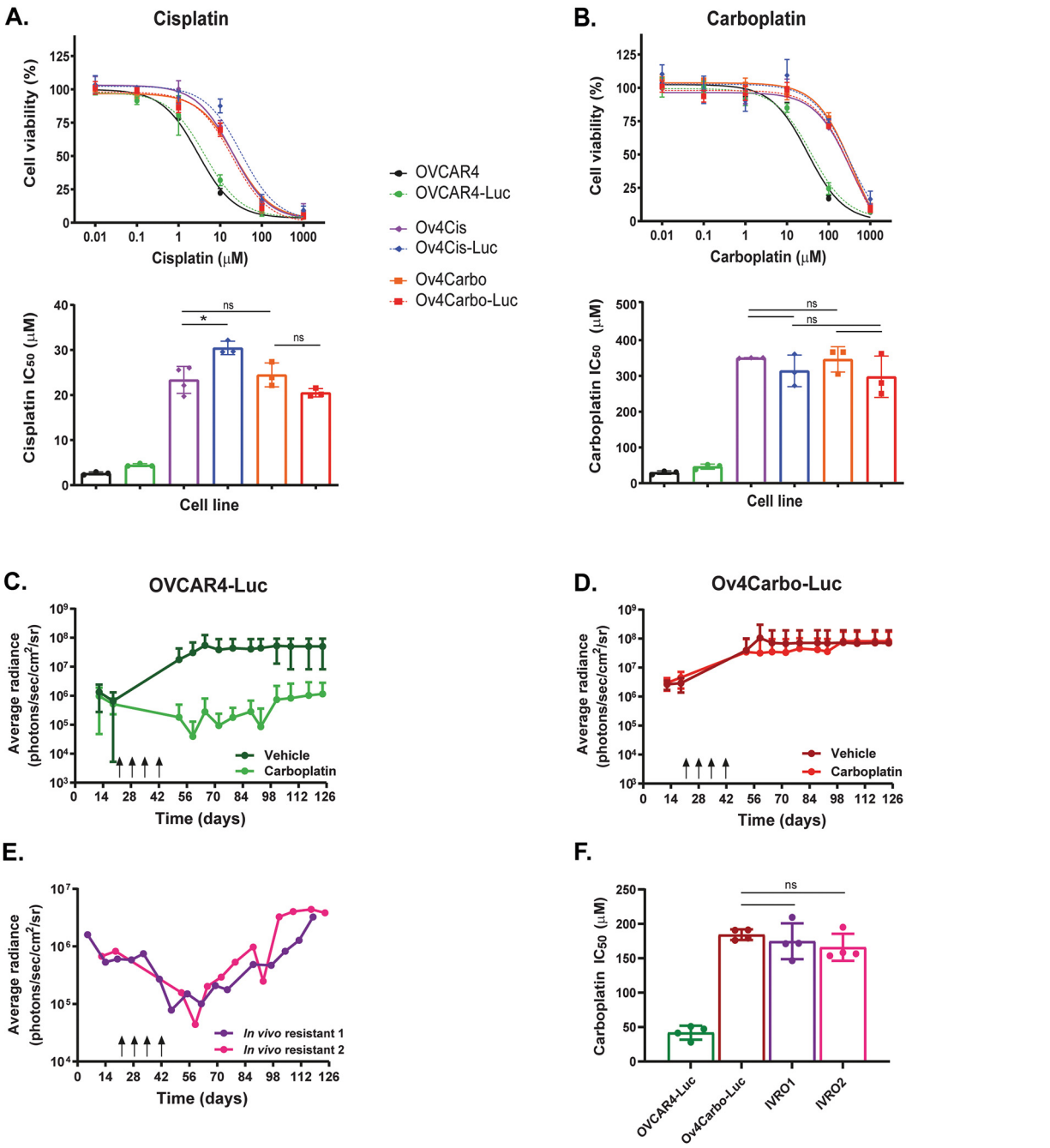

Fig. 2. Platinum resistance is comparable whether it is induced by cisplatin or carboplatin, *in vitro* or *in vivo*.
In vitro dose response curves and IC50 to A. cisplatin and B. carboplatin by MTT assay 72 h after drug administration. Black = OVCAR4, Green = OVCAR4-Luc, purple = Ov4Cis, blue = Ov4Cis-Luc, orange = Ov4Carbo, red = Ov4Carbo-Luc. $N = 3$, mean ± s.d., unpaired *t*-test, ns = non-significant, $^{*}P < 0.05$. Female CD1*nu/nu* mice with intraperitoneal (IP) xenografts of either C. OVCAR4-Luc or D. Ov4Carbo-luc cells. Mice were treated IP with either carboplatin 50 mg/kg or vehicle control on days 21, 28, 35 and 42 (black arrows). Average radiance (photons/s/cm^2/sr) is shown over time. C. Dark green = vehicle-treated OVCAR4-Luc xenografts, light green = carboplatin-treated OVCAR4-Luc xenografts, D. dark red = vehicle-treated Ov4Carbo-Luc xenografts, light red = carboplatin-treated Ov4Carbo-Luc xenografts. $N = 4$–5 per group, mean ± s.d. E. At Home Office end point OVCAR4-Luc tumours were harvested from two separate mice that had both received carboplatin. Light output from these two mice over time is shown. Tumours were homogenized and cells cultured *in vitro* to create the carboplatin-resistant cell lines, IVR01 (purple: *in vivo* resistant 1) and IVR02 (pink: *in vivo* resistant 2). **F.** IC_{50} to carboplatin by CTG at 72 h. $N = 4$, mean ± s.d., ns = non-significant.

Next we conducted pathway analysis of the gene expression changes that occurred in ICGC resistant/refractory human samples and also in each of our resistant cell lines (Ov4Carbo: Fig. 4C and Ov4Cis: Fig. 4D), compared to their sensitive counterparts. The most significantly over-represented pathway was 'extracellular matrix organisation' and 'extracellular matrix disassembly' was also over-represented in both cell lines (Fig. 4C-D and Supplementary Table 2, hypergeometric test, adjusted $P < 0.05$). 16 ECM genes were significantly differentially expressed in both resistant cell lines and in resistant human samples (Fig. 4E). We did not identify mutations in any of these common ECM genes and only one (MMP1) showed concordant change in copy number in Ov4Carbo cells (full list of resistance-associated copy number alterations (CNAs) overlaid with RNASeq in Supplementary Table 3). We validated two of these ECM genes; IL-6 and TNF using an

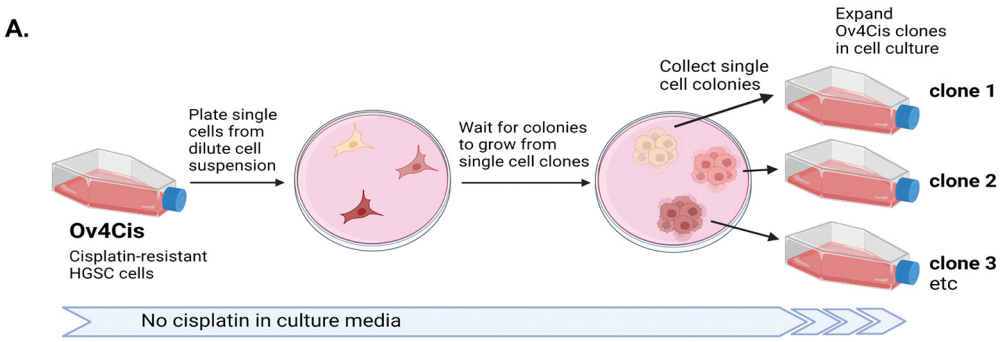

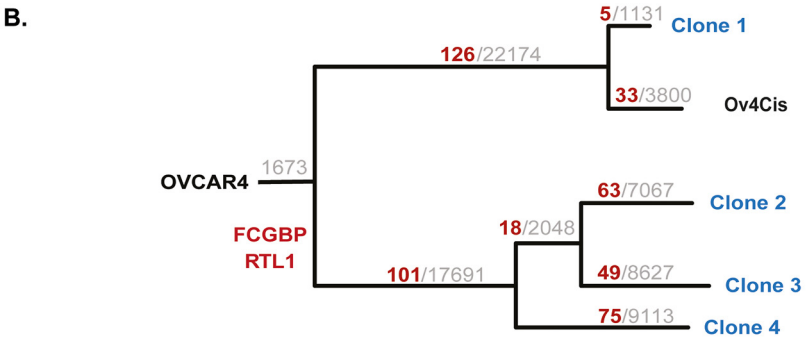

OVCAR4 = platinum sensitive
Ov4Cis = cisplatin resistant, derived from OVCAR4
Clone 1, 2, 3, 4 = single cell clones derived from Ov4Cis

Red = non-synonymous exonic variant with VAF >0.1
Grey = synonymous exonic variants with VAF >0.1

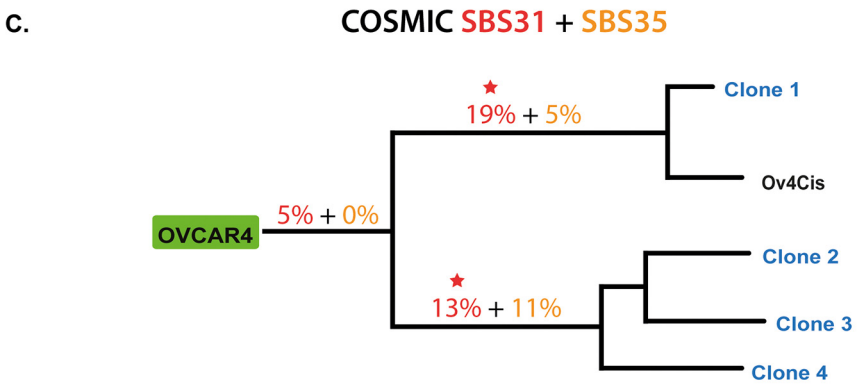

Red = COSMIC platinum chemotherapy-associated signature SBS31
Orange = COSMIC platinum chemotherapy-associated signature SBS35
% = estimated contribution of signatures to shared mutations in respective area of phylogentic tree
* = COSMIC signature with the largest proportional contribution of all COSMIC signatures to that mutational profile

Fig. 3. Whole genome sequencing of cisplatin-resistant HGSC cells indicates evolution from a pre-existing ancestral clone.
A. Schematic describing creation of Ov4Cis clones B. Deep whole genome sequencing (50× mean depth, Illumina's HiSeq X Ten) of OVCAR4, Ov4Cis and four cell lines derived from single Ov4Cis clones (clones 1–4). Red = number of non-synonymous exonic variant with variant allele frequency > 0.1, grey = number of synonymous exonic variant with variant allele frequency > 0.1. C. Proportional contribution of COSMIC platinum chemotherapy-associated signatures SBS31 and SBS35 to clonal mutations and mutations carried by cells in the two main lineages. Values marked with a star indicate the COSMIC signature with the largest proportional contribution of all COSMIC signatures to that mutational profile.

ELISA-based electrochemiluminscent system (MesoScale Diagnostics, LLC®) and demonstrated that reduced expression by RNASeq (Fig. 4E) was reflected in reduced protein production (Fig. 4F). These comparisons therefore reveal candidate genes and pathways that could be further interrogated using these cell line models.

2.5. Extracellular matrix gene-expression pathways are over-represented in multiple resistant settings

ECM is known to control cancer cell growth, invasion and survival [16]. Clinically, it is associated with metastasis, disease progression [27] and drug resistance [28]. Our discovery of ECM pathway upregulation in resistant epithelial cancer cells suggests that the cancer cells themselves modulate the extracellular matrix (ECM) during the evolution of platinum-resistance. We used our comparison between the transcriptome of the two resistant cell lines (Ov4Carbo and Ov4Cis) and sensitive, ancestral OVCAR4 cells to explore this hypothesis. Principal component analysis (Supplementary Fig. S1A) and unsupervised hierarchical cluster analyses (Supplementary Fig. S1B) resulted in a clear segregation of the three sample groups. (Supplementary Fig. S1C: number of genes, Supplementary Fig. S1D: Venn diagrams, Supplementary Fig. S1E: heatmaps. Supplementary Table 4). Gene Ontology Biological Process (GOBP) enrichment analysis was conducted (Supplementary Table 5) and the ten most significant pathways in each comparison are shown in Fig. 5A.

Several pathways were significant in the intersect of both resistant cell lines compared to OVCAR4 (Fig. 5A, left). These shared pathways could represent resistance mechanisms that are utilised by both Ov4Carbo and Ov4Cis cells and might explain the overlapping resistance to cisplatin and carboplatin previously observed (Fig. 2A-B). Certain pathways were significant both in the intersect of the two resistant cell lines and also in different genes that were unique to each cell line. For example 'axon guidance' and 'cell adhesion' were found in the intersect and in genes unique to Ov4Carbo (Fig. 5A, yellow shade) while 'angiogenesis' was significant in the intersect and in genes unique to Ov4Cis (Fig. 5A, lilac shade). These recurrent pathways therefore appear to be specifically advantageous to each cell line during the evolution of platinum resistance.

'Extracellular matrix organisation' and 'extracellular matrix disassembly' were again significant in the intersect of both resistant cell lines compared to OVCAR4 (Fig. 5A, left and Supplementary Table 5A). Interestingly, 'extracellular matrix organisation' was also found in additional sets of genes that were unique to Ov4Carbo cells (Fig. 5A, middle and Supplementary Table 5B) and in yet another set of genes that were unique to Ov4Cis cells (Fig. 5A, right and Supplementary Table 5C). This repeated enrichment of ECM pathways by distinct sets of differentially expressed genes hints at a convergent evolutionary process by which modulation of the ECM may provide a strong and context-independent fitness advantage as platinum-resistant HGSC evolves in different cell lines and also in human patients.

2.6. Platinum-resistant cell lines evolve diverse intraperitoneal phenotypes

We next explored the *in vivo* role of the gene expression pathways that had evolved in our resistant cell lines. Female nude mice were injected IP with either OVCAR4-Luc, Ov4Cis-Luc and Ov4Carbo-Luc cells and monitored with weekly bioluminescence imaging (BLI). For scientific rigour, all experiments that we have conducted to date are included here. Median survival (time to reach humane endpoint) of OVCAR4-Luc mice was 100 days. Ov4Carbo-Luc cells had a reduced median survival of 56 days. In contrast, no mice with IP Ov4Cis-Luc xenografts had reached humane endpoint at 140 days (log-rank test $P < 0.001$) (Fig. 5B). Survival differences were reflected in BLI over time (Fig. 5C).

Post-mortem examination revealed that OVCAR4-Luc and Ov4Carbo-Luc IP tumours mirrored the most common manifestation of the human disease with multiple, peritoneal nodules and ascites (Fig. 5D). Ov4Cis-Luc tumours on the other hand formed discrete peritoneal tumour nodules (Fig. 5D). Pathological examination revealed that Ov4Cis-Luc nodules consisted of a rim of tumour surrounding a central necrotic core while Ov4Carbo-Luc tumours invaded local structures (Fig. 5E). Ov4Carbo-Luc xenografts had the highest measured tumour weight at necropsy, although there was wide variation (Supplementary Fig. S2A). Three mice in each group produced no ascites at all (60% Ov4Cis mice; 14% Ov4Carbo; 33% OVCAR4) and although OVCAR4 mice appeared to produce the greatest amount of ascites (Supplementary Fig. S2B) there was no statistical difference between the three models. Potential differences will be resolved *via* future experiments enrolling a greater number of animals.

Thus despite their overlapping resistance to cisplatin (Fig. 2A) and carboplatin (Fig. 2B), Ov4Carbo behaved more aggressively while Ov4Cis cells were markedly less invasive *in vivo* with a much more indolent clinical course. The unique transcriptional pathways that these cell lines evolved under drug pressure (Fig. 5A) could explain their very different *in vivo* behaviour. Moreover, transcriptomic and clinical overlap with resistant human HGSC, indicates that these resistant cell lines could be used as an accurate experimental platform to interrogate the evolution of platinum-resistant human HGSC.

3. Discussion

Drug resistance remains a major obstacle in cancer care and progress in HGSC has been hindered by the paucity of representative pre-clinical models. Our platinum-resistant HGSC cell lines have the advantage that they are readily cultured in standard laboratory conditions, have been rigorously maintained at very low passage and are now freely available [29]. Resistant cells that we derived in the peritoneal environment are predicted to be particularly informative. Our cell lines accurately reflect the diverse clinical phenotypes and disease trajectories that can occur in patients with relapsed HGSC [30]. The infiltrative and metastatic intraperitoneal phenotype produced by Ov4Carbo cells is analogous to the most usual pattern of recurrent, human HGSC [4]. In contrast Ov4Cis cells produced a less aggressive *in vivo* phenotype. This could be explained as a fitness cost of resistance, which has been observed and exploited therapeutically in cancer patients [31]. Importantly, the oligo-metastatic picture of Ov4Cis cells focused on localised disease, lymph node metastasis and a favourable outcome also occurs in human HGSC [5].

Genetic evolution has long been considered central to drug resistance. In HGSC, the frequency of recurrent oncogenic mutations is low and as expected from existing data [2,15,16] we did not identify a unifying mutational cause for platinum resistance. Only two nonsynonymous mutations were common to all five of the cisplatin-resistant cells tested and although one of these genes, *FCGBP*, has previously been linked to chemotherapy resistance [32,33] this gene was not expressed in our RNASeq analysis.

There was however, significant overlap in the gene expression changes that evolved in our cell lines and human resistant HGSC, implicating non-genetic factors in mediating therapeutic evasion. This is in keeping with a growing literature describing cancer therapy resistance in the absence of an obvious genetic cause (reviewed in [34]). Although a limitation of our study is that resistant cell lines were only evolved once in each experimental condition, our demonstration of transcriptional overlap with multiple resistant human HGSC samples in three independent datasets, strongly implies that the reproducible features we identified are relevant to patients.

We have previously described evolution of a common matrix response that correlates with patient outcome in multiple cancers including HGSC [27] and platinum chemotherapy has recently been shown to influence the dynamic interaction between cancer cells and the ECM in HGSC [28]. The ECM pathways we repeatedly identified using cancer cell lines, therefore raises the intriguing possibility that cancer

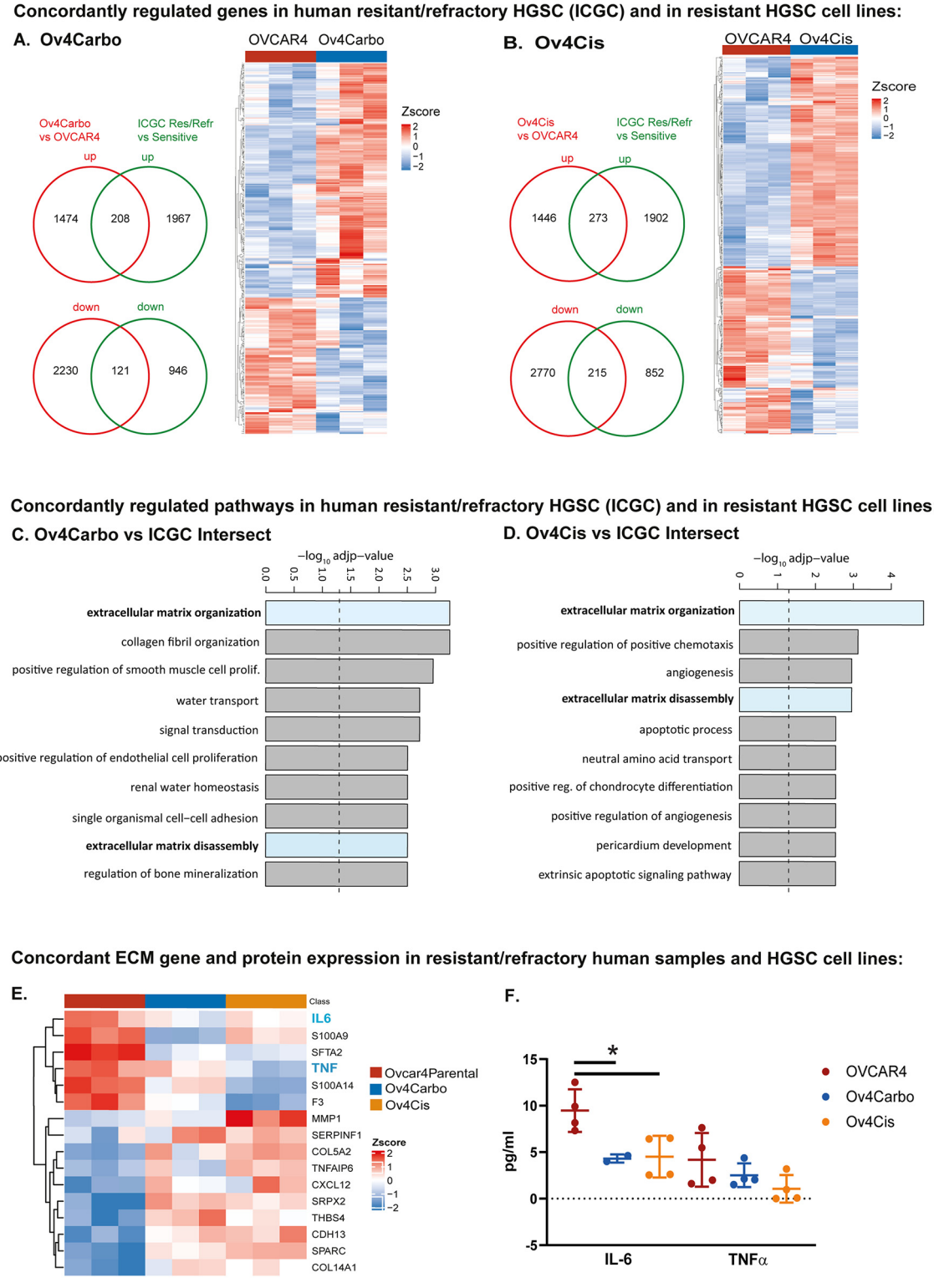

Fig. 4. Platinum-resistant OVCAR4-derived clones share multiple transcriptional features with platinum resistant/refractory human HGSC.
Venn diagrams and heatmaps illustrating the differentially expressed protein-coding genes in A. Ov4Carbo *vs.* OVCAR4 Parental and B. Ov4Cis *vs.* OVCAR4 Parental and their overlap with gene expression differences between human resistant/refractory HGSC ($N = 49$) and sensitive HGSC ($N = 31$) obtained from the ICGC dataset. The 10 most significant Gene Ontology Biological Processes (GOBP) in C. ICGC resistant/refractory *vs.* sensitive human HGSC and also resistant Ov4Carbo *vs.* sensitive OVCAR4 cell lines and D. ICGC resistant/refractory *vs.* sensitive human HGSC and also resistant Ov4Cis *vs.* sensitive OVCAR4 cell lines. E. Heatmap illustrating ECM genes with significantly different expression in ICGC resistant/refractory *vs.* sensitive human HGSC and also resistant *vs.* sensitive OVCAR4-derived cell lines. F. Quantification of IL-6 and TNFa proteins in cell culture supernatant. $N = 2$–4 per group, mean ± s.d.

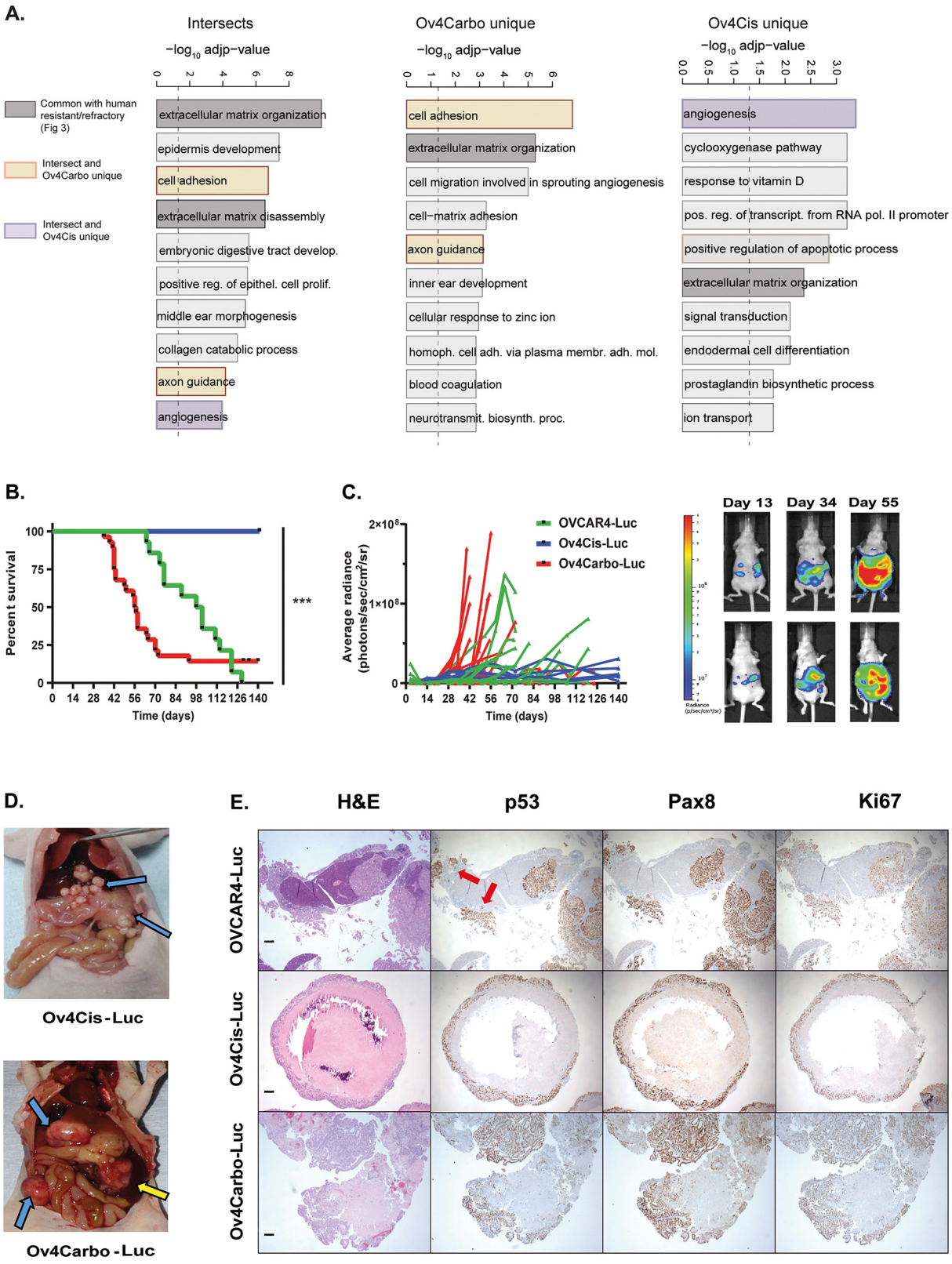

Fig. 5. Platinum-resistance produces diverse intraperitoneal phenotypes

A. Gene Ontology Biological Process enrichment analysis of the intersect genes, the uniquely DE in the Ov4Carbo *vs* OVCAR4 and the uniquely DE in the Ov4Cis *vs* OVCAR4. B. Kaplan Meier survival curves of untreated mice with IP OVCAR4-Luc, Ov4Cis-Luc or Ov4Carbo-Luc xenografts in female CD1*nu/nu* mice. Green = OVCAR4-Luc ($N = 14$), red = Ov4Carbo-Luc ($N = 28$), blue = Ov4Cis-Luc ($N = 5$) $^{***}P < 0.001$, log-rank test. C. Corresponding light output (BLI) and representative images (Ov4Carbo-Luc) in untreated mice are shown over time. D. Macroscopic images in Ov4Cis-Luc and Ov4Carbo-Luc xenografts taken at necropsy. Ov4Cis-Luc xenografts remained localised, creating multiple small nodules (blue arrows) without invasion of other organs. Ov4Carbo-Luc produced multiple peritoneal nodules (blue arrows) and haemorrhagic ascites (yellow arrows). E. Pathological examination (H + E and IHC) demonstrating that OVCAR4-Luc and Ov4Carbo-Luc invade local structures (red arrows) whereas Ov4Cis-Luc remains localised in tumour nodules with a necrotic core. Positive staining for p53, the Mullerian transcription factor PAX8, and Ki67 are shown. Scale bars = 200 μm.

cell-intrinsic mechanisms could in fact direct adaptation of the ECM during the evolution of chemotherapy resistance. Moreover, our observation that the GOBP pathway 'extracellular matrix organisation' was enriched by distinct sets of genes in all resistant settings, implies a convergent evolutionary process supporting a role for the ECM in therapeutic evasion that occurs in human HGSC and can now be effectively modelled using Ov4Cis and Ov4Carbo cells.

In summary, we have created a unique and usable panel of platinum-resistant HGSC cells lines that reflect the human disease. We have discovered that specific transcriptional alterations are associated with overlapping resistance in multiple disease contexts. These coexist with a distinct repertoire of transcriptional changes that mediate phenotypic diversity, echoing human cancer. Intriguingly, our findings hint at convergent evolution during platinum resistance since specific biological pathways, most notably those associated with the ECM, are conserved *via* expression of different genes in multiple resistant HGSC cell lines and human patients. We anticipate that further interrogation of our cell panel and the role of these resistance-associated biological pathways, could potentially reveal new biological insights and therapeutic opportunities in platinum-resistant HGSC.

4. Methods

4.1. Cell culture and chemotherapy-resistant cell lines

Human HGSC cell lines OVCAR4, Cov318 and Ovsaho were obtained from Prof Fran Balkwill (Barts Cancer Institute, UK) and grown in DMEM (OVCAR4, Cov318) or RPMI (Ovsaho) containing 10% FBS and 1% penicillin/streptomycin. Platinum-resistant HGSC lines were generated by culturing cells in increasing concentrations of cisplatin (to create Ov4Cis, CovCis, OvsahoCis) or carboplatin (to create Ov4Carbo, CovCarbo, OvsahoCarbo) until IC_{50} increased by 2–10 fold. Cells were immediately bulked and stored at -80 °C. Original stocks were used at low passage in all subsequent experiments and are deposited in Ximbio [29]. To create single cell clones, Ov4Cis cells were cultured without cisplatin at low densities in 10 cm plates. Single cells were identified and plates monitored daily by light microscopy. Colonies growing from single cells were harvested and bulked to establish four separate clones: 1, 2, 3 and 4. All cell lines underwent 16 locus STR verification (European Collection of Authenticated Cell Lines August 2019) and routine mycoplasma testing.

4.2. In vitro experiments

Cell viability was assessed using either MTT (Thiazolyl Blue Tetrazolium Bromide, AlfaAesar, 5 mg/ml) or CTG (CellTiter-Glo®, Promega). MTT crystals were dissolved in DMSO after two hours incubation at 37 °C and absorbance measured using a Perkin-Elmer plate reader. For CTG, light emission was quantified using a Perkin-Elmer plate reader. Secreted proteins (IL-6 and TNF) were quantified in culture supernatants (duplicate wells per sample) using the U-PLEX Biomarker Group 1 (hu) assays kit (MesoScale Diagnostics, LLC®). Data were analysed using DISCOVERY WORKBENCH® 4.0 software.

4.3. Luminescent and fluorescent reporters

OVCAR4 cells were treated with lentiviral particles (MOI 10) containing dual constructs of green fluorescent protein (GFP) and Firefly luciferase (CMV-Luciferase (firefly)-2A-GFP (Puro)) to create OVCAR4-Luc. Ov4Cis and Ov4Carbo cells were treated with lentiviral particles (MOI 10) containing dual constructs of red fluorescent protein (RFP) and Firefly luciferase (CMV-Luciferase (firefly)-2A-RFP (Puro)) (AMS Biotechnology®) to create Ov4Cis-Luc and Ov4Carbo-Luc. Transfected cells were cultured in puromycin-containing media (0.9 μg/mL).

4.4. Animal studies

Approval was obtained from the Institutional Review Board at Barts Cancer Institute, Queen Mary University of London under project licence P1EE3ECB4, as required by the UK government Home Office in accordance with the Animals (Scientific Procedures) Act 1986 (ASPA). Investigators were blind to experimental groups. Cells were inoculated by intraperitoneal (IP) injection (5×10^6 cells/200 μl sterile PBS) in female CD1*nu*/*nu* mice (Charles River Laboratories). Animals received D-Luciferin monopotassium salt (ThermoFisher) 3.7 mg/200 μl PBS IP. Light emission was recorded using an IVIS® Spectrum (PerkinElmer) and analysed using Living Image® v7.4.2. Mice were assessed for weight, general health, and accumulation of ascites and were killed according to UK Home Office guidelines. At necropsy, murine tissue was fixed in 10% formaldehyde and paraffin-embedded. 4 μm sections were stained with H + E and by IHC for p53 (DAKO IS616), Pax8 (Abcam ab181054) and Ki67 (Abcam ab15580).

4.5. Production of ex-vivo cell lines

IP tumours were minced with a scalpel in ice-cold PBS and digested using collagenase type I (Fisher, 1 mg/ml in 5% FCS/PBS). Tissues were incubated at 37 °C with shaking (90 rpm, ≥60mins), strained through a 70 μm filter, washed and plated in DMEM +10% FCS and 1% penicillin/streptomycin.

4.6. DNA extraction and deep whole genome sequencing (dWGS)

DNA was extracted using a QIamp DNA Blood Mini Kit (Qiagen). DNA quantity was evaluated using the Qubit 4 Fluorometer (Invitrogen™) then sonicated to fragments of 300-400 bp using the M220 focused ultrasonicator (Covaris). Sequencing libraries were prepared using the NEBNext Ultra kit (New England Biolabs) using 300 ng fragmented DNA input for each sample. Libraries were sequenced to a target coverage of 50× on Illumina's HiSeq X Ten platform (150 bp paired end reads).

Platypus was used for variant calling of point mutations by comparison to the human reference genome (hg19). Mutations were considered if the coverage depth was ≥10. Mutations present in resistant but not the parental sensitive sample (OVCAR4) were used to construct a phylogenetic tree using maximum parsimony. Nonsynonymous and synonymous exonic mutations were annotated using Annovar. Data available at GitHub: https://github.com/WeiniHuangBW/OvarianCancerCellLines.

Mutational signature analysis of point mutations in resistant samples was conducted using the R package MutationalPatterns [35] with the COSMIC signature library (COSMIC v3.1, available at https://cancer.sanger.ac.uk/cosmic/signatures/SBS/index.tt). The contribution of all 72 COSMIC signatures to the sample mutational profiles was first estimated, and subsequently the 7 highest contributing signatures were re-fitted to the sample profiles (Supplementary Fig. S3A–B). Pairwise similarity of each of the top 7 COSMIC signatures to the sample mutational profiles was characterised by computing the cosine similarity (Supplementary Fig. S3C).

4.7. RNA Sequencing and bioinformatics analysis

RNA was extracted using the Qiagen RNeasy kit according to the manufacturer's instructions. RNA was quantified by NanoDrop™ spectrophotometer (Thermo) and quality determined on the Agilent Bioanalyzer 2100 using RNA Nano Chips. Library prep and RNA sequencing were carried out by the Oxford Genomics Centre (Wellcome Centre for Human Genetics, Oxford) using PolyA capture. Sequencing was performed to ~32× mean depth on the Illumina HiSeq4000 platform, strand-specific, generating 75 bp paired-end reads. RNASeq samples were mapped to the human genome (hg19, Genome Reference Consortium GRCh37) in strand-specific mode as part of the Wellcome

Trust Centre pipeline. Number of reads aligned to the exonic region of each gene were counted using htseq-count based on the Ensembl annotation. Only genes that achieved at least one read count per million reads (cpm) in at least 25 % of the samples were kept. Conditional quantile normalization [36] was performed accounting for gene length and GC content and a $\log_2$-transformed RPKM expression matrix was generated. Differential expression analysis was performed in EdgeR using the 'limma' R package [37]. Gene clusters segregating multiple sample classes were identified using the function sam from R package siggenes. Gene-set enrichment analysis (GSEA) was performed using the GSEA software [38] to identify dysregulated canonical pathways curated in the Molecular Signatures Database (MSigDB-C2-CP v6.2). Pathway enrichment analysis was performed using R package dnet. RNA-Seq data have been deposited in Gene Expression Omnibus (GEO) under the accession number GSE141630.

The ICGC_OV read counts were extracted from the exp_seq.OV-AU.tsv.gz file in the ICGC data repository Release 20 [24]. Only genes that achieved at least one read count in at least ten samples were selected, producing 18,010 filtered genes in total and voom normalization was applied. Differential expression analysis was performed in EdgeR comparing platinum resistant plus refractory ($N = 49$) *versus* sensitive ($N = 31$) donor samples. All graphics and statistical analyses were performed in the statistical programming language).

4.8. Statistical analysis

Data are presented as mean ± s.d. Normal distribution was tested using the Shapiro-Wilk normality test. Statistical significance was calculated using a two-tailed unpaired *t*-test unless otherwise specified ($^{*}P < 0.05$; $^{**}P < 0.001$; $^{***}P < 0.0001$). *n* refers to biological replicates and the established scientific standard of $n \geq 3$ was applied throughout. Dose-response curves, IC_{50} values and statistical analysis were performed using GraphPad Prism v.8.0. All analysis and plots from sequencing data were generated in R (versions 3.1.3 and 4.0.1).

Funding

ML, JIH and FN were supported by ML's Cancer Research UK Advanced Clinician Scientist Fellowship (C41405/A19694). ML and JIH received support from the Barts Cancer Institute Impetus Fund. ML and AB received support from ML's Cancer Research UK Clinician Scientist Fellowship (C41405/A13034). ML, JS and *VS* were supported by a Barts and The London Charity Strategic Research Grant (467/2244). HH was supported by a CRUK Clinical Research Training Fellowship (S_3398) and GEW was supported by Barts and The London Charity Clinical Research Training Fellowships (MGU0370 and MGU0469).

CRediT authorship contribution statement

J.I. Hoare: Methodology, Validation, Formal analysis, Investigation, Writing – review & editing, Visualization. **H. Hockings:** Methodology, Validation, Formal analysis, Investigation, Writing – review & editing, Visualization. **J. Saxena:** Methodology, Validation, Formal analysis, Investigation, Writing – review & editing, Visualization. **V.L. Silva:** Methodology, Validation, Formal analysis, Investigation, Writing – review & editing, Visualization. **M.J. Haughey:** Methodology, Software, Validation, Formal analysis, Investigation, Resources, Data curation, Writing – review & editing, Visualization. **G.E. Wood:** Methodology, Validation, Formal analysis, Investigation, Writing – review & editing, Visualization. **F. Nicolini:** Methodology, Validation, Formal analysis, Investigation, Writing – review & editing, Visualization. **H. Mirza:** Software, Validation, Formal analysis, Investigation, Resources, Data curation, Writing – review & editing. **I.A. McNeish:** Conceptualization, Resources, Data curation, Writing – original draft, Writing – review & editing, Supervision. **W. Huang:** Software, Resources, Data curation, Writing – review & editing, Supervision. **E. Maniati:** Software, Investigation, Resources, Data curation, Writing – original draft, Writing – review & editing, Visualization. **T.A. Graham:** Conceptualization, Resources, Data curation, Writing – original draft, Writing – review & editing, Supervision. **M. Lockley:** Conceptualization, Methodology, Software, Validation, Formal analysis, Investigation, Resources, Data curation, Writing – original draft, Writing – review & editing, Visualization, Supervision, Project administration, Funding acquisition.

Declaration of Competing Interest

The authors declare no conflicts of interest.

Acknowledgements

We thank Ashley Browne for originally creating OVCAR4-Luc, Ov4Cis, Ov4Cis-Luc, Ov4Carbo, Ov4Carbo-Luc, CovCis and OvsahoCis, Jacqueline McDermott for interpretation of pathology slides, Cheng Zhao and Ann-Marie Baker for experimental and logistic contributions to whole genome sequencing and to Prof Tyson Sharp, Dr. Sarah Martin and Dr. Sarah McClelland for reviewing and advising on this manuscript.

Appendix A. Supplementary data

Supplementary data to this article can be found online at https://doi.org/10.1016/j.ygyno.2022.07.027.

References

[1] W.G. McCluggage, Morphological subtypes of ovarian carcinoma: a review with emphasis on new developments and pathogenesis, Pathology. 43 (5) (2011) 420–432.
[2] D.D. Bowtell, S. Bohm, A.A. Ahmed, P.J. Aspuria, R.C. Bast Jr., V. Beral, et al., Rethinking ovarian cancer II: reducing mortality from high-grade serous ovarian cancer, Nat. Rev. Cancer 15 (11) (2015) 668–679.
[3] G.C. Jayson, E.C. Kohn, H.C. Kitchener, J.A. Ledermann, Ovarian cancer, Lancet. 384 (9951) (2014) 1376–1388.
[4] P. Amate, C. Huchon, A.L. Dessapt, C. Bensaid, J. Medioni, M.A. Le Frere Belda, et al., Ovarian cancer: sites of recurrence, Int. J. Gynecol. Cancer 23 (9) (2013) 1590–1596.
[5] R.L. Hollis, J. Carmichael, A.M. Meynert, M. Churchman, A. Hallas-Potts, T. Rye, et al., Clinical and molecular characterization of ovarian carcinoma displaying isolated lymph node relapse, Am. J. Obstet. Gynecol. 221 (3) (2019) 245 e1- e15.
[6] N. Colombo, C. Sessa, A. du Bois, J. Ledermann, W.G. McCluggage, I. McNeish, et al., ESMO-ESGO consensus conference recommendations on ovarian cancer: pathology and molecular biology, early and advanced stages, borderline tumours and recurrent diseasedagger, Ann. Oncol. 30 (5) (2019) 672–705.
[7] I.A. McNeish, J.A. Ledermann, L. Webber, L. James, S.B. Kaye, M. Hall, et al., A randomised, placebo-controlled trial of weekly paclitaxel and saracatinib (AZD0530) in platinum-resistant ovarian, fallopian tube or primary peritoneal cancerdagger, Ann. Oncol. 25 (10) (2014) 1988–1995.
[8] E. Pujade-Lauraine, F. Hilpert, B. Weber, A. Reuss, A. Poveda, G. Kristensen, et al., Bevacizumab combined with chemotherapy for platinum-resistant recurrent ovarian cancer: the AURELIA open-label randomized phase III trial, J. Clin. Oncol. 32 (13) (2014) 1302–1308.
[9] J. Ledermann, P. Harter, C. Gourley, M. Friedlander, I. Vergote, G. Rustin, et al., Olaparib maintenance therapy in platinum-sensitive relapsed ovarian cancer, N. Engl. J. Med. 366 (15) (2012) 1382–1392.
[10] R.L. Coleman, A.M. Oza, D. Lorusso, C. Aghajanian, A. Oaknin, A. Dean, et al., Rucaparib maintenance treatment for recurrent ovarian carcinoma after response to platinum therapy (ARIEL3): a randomised, double-blind, placebo-controlled, phase 3 trial, Lancet. 390 (10106) (2017) 1949–1961.
[11] M.R. Mirza, B.J. Monk, J. Herrstedt, A.M. Oza, S. Mahner, A. Redondo, et al., Niraparib maintenance therapy in platinum-sensitive, recurrent ovarian Cancer, N. Engl. J. Med. 375 (22) (2016) 2154–2164.
[12] K. Moore, N. Colombo, G. Scambia, B.G. Kim, A. Oaknin, M. Friedlander, et al., Maintenance Olaparib in patients with newly diagnosed advanced ovarian Cancer, N. Engl. J. Med. 379 (26) (2018) 2495–2505.
[13] A. Gonzalez-Martin, B. Pothuri, I. Vergote, Christensen R. DePont, W. Graybill, M.R. Mirza, et al., Niraparib in patients with newly diagnosed advanced ovarian Cancer, N. Engl. J. Med. 381 (25) (2019) 2391–2402, https://doi.org/10.1056/NEJMoa1910962.
[14] R.L. Coleman, G.F. Fleming, M.F. Brady, E.M. Swisher, K.D. Steffensen, M. Friedlander, et al., Veliparib with first-line chemotherapy and as maintenance therapy in ovarian Cancer, N. Engl. J. Med. 381 (25) (2019) 2403–2415, https://doi.org/10.1056/NEJMoa1909707.
[15] M. Javellina, M.A. Eckert, J. Heide, K. Zawieracz, M. Weigert, S. Ashley, E. Stock, D. Chapel, L. Huang, D. Yamada, A.A. Ahmed, R.R. Lastra, M. Chen, E. Lengyel, et al., Neoadjuvant CHemo er, Cancer Res. 82 (1) (2022) 169–176, https://doi.org/10.1158/0008-5472.

[16] G. Macintyre, T.E. Goranova, D. De Silva, D. Ennis, A.M. Piskorz, M. Eldridge, et al., Copy number signatures and mutational processes in ovarian carcinoma, Nat. Genet. 50 (9) (2018) 1262–1270.
[17] T.A. Ince, A.D. Sousa, M.A. Jones, J.C. Harrell, E.S. Agoston, M. Krohn, et al., Characterization of twenty-five ovarian tumour cell lines that phenocopy primary tumours, Nat. Commun. 6 (2015) 7419.
[18] L. Nelson, A. Tighe, A. Golder, S. Littler, B. Bakker, D. Moralli, et al., A living biobank of ovarian cancer ex vivo models reveals profound mitotic heterogeneity, Nat. Commun. 11 (1) (2020) 822.
[19] S. Domcke, R. Sinha, D.A. Levine, C. Sander, N. Schultz, Evaluating cell lines as tumour models by comparison of genomic profiles, Nat. Commun. 4 (2013) 2126.
[20] Z. Duan, A.J. Feller, R.T. Penson, B.A. Chabner, M.V. Seiden, Discovery of differentially expressed genes associated with paclitaxel resistance using cDNA array technology: analysis of interleukin (IL) 6, IL-8, and monocyte chemotactic protein 1 in the paclitaxel-resistant phenotype, Clin. Cancer Res. 5 (11) (1999) 3445–3453.
[21] K.M. Elias, M.M. Emori, E. Papp, E. MacDuffie, G.E. Konecny, V.E. Velculescu, et al., Beyond genomics: critical evaluation of cell line utility for ovarian cancer research, Gynecol. Oncol. 139 (1) (2015) 97–103.
[22] A.K. Mitra, D.A. Davis, S. Tomar, L. Roy, H. Gurler, J. Xie, et al., In vivo tumor growth of high-grade serous ovarian cancer cell lines, Gynecol. Oncol. 138 (2) (2015) 372–377.
[23] M. McDermott, A.J. Eustace, S. Busschots, L. Breen, J. Crown, M. Clynes, et al., In vitro development of chemotherapy and targeted therapy drug-resistant Cancer cell lines: A practical guide with case studies, Front. Oncol. 4 (2014) 40.
[24] ICGC, ICGC Data Portal, Available from: http://dcc.icgc.org 2019.
[25] M. Artibani, K. Masuda, Z. Hu, P.C. Rauher, G. Mallett, N. Wietek, et al., Adipocyte-like signature in ovarian cancer minimal residual disease identifies metabolic vulnerabilities of tumor-initiating cells. JCI, Insight. 6 (11) (2021).
[26] J.F. Hastings, J.N. Skhinas, D. Fey, D.R. Croucher, T.R. Cox, The extracellular matrix as a key regulator of intracellular signalling networks, Br. J. Pharmacol. 176 (1) (2019) 82–92.
[27] O.M.T. Pearce, R.M. Delaine-Smith, E. Maniati, S. Nichols, J. Wang, S. Bohm, et al., Deconstruction of a metastatic tumor microenvironment reveals a common matrix response in human cancers, Cancer Discov. 8 (3) (2018) 304–319.
[28] E.A. Pietila, J. Gonzalez-Molina, L. Moyano-Galceran, S. Jamalzadeh, K. Zhang, L. Lehtinen, et al., Co-evolution of matrisome and adaptive adhesion dynamics drives ovarian cancer chemoresistance, Nat. Commun. 12 (1) (2021) 3904.
[29] Ximbio, https://ximbio.com/ 2020.
[30] S. Pignata, S CC, Du Bois A, Harter P, Heitz F., Treatment of recurrent ovarian cancer, Ann. Oncol. 28 (suppl_8) (2017) viii51-viii6.
[31] J. Zhang, J. Cunningham, J. Brown, R. Gatenby, Evolution-based mathematical models significantly prolong response to abiraterone in metastatic castrate-resistant prostate cancer and identify strategies to further improve outcomes, Elife. 11 (2022).
[32] C.H. Choi, J.J. Choi, Y.A. Park, Y.Y. Lee, S.Y. Song, C.O. Sung, et al., Identification of differentially expressed genes according to chemosensitivity in advanced ovarian serous adenocarcinomas: expression of GRIA2 predicts better survival, Br. J. Cancer 107 (1) (2012) 91–99.
[33] Y. Gao, X. Liu, T. Li, L. Wei, A. Yang, Y. Lu, et al., Cross-validation of genes potentially associated with overall survival and drug resistance in ovarian cancer, Oncol. Rep. 37 (5) (2017) 3084–3092.
[34] J.C. Marine, S.J. Dawson, M.A. Dawson, Non-genetic mechanisms of therapeutic resistance in cancer, Nat. Rev. Cancer 20 (12) (2020) 743–756.
[35] F. Blokzijl, R. Janssen, R. van Boxtel, E. Cuppen, MutationalPatterns: comprehensive genome-wide analysis of mutational processes, Genome Med. 10 (1) (2018) 33.
[36] K.D. Hansen, R.A. Irizarry, Z. Wu, Removing technical variability in RNA-seq data using conditional quantile normalization, Biostatistics. 13 (2) (2012) 204–216.
[37] M.E. Ritchie, B. Phipson, D. Wu, Y. Hu, C.W. Law, W. Shi, et al., Limma powers differential expression analyses for RNA-sequencing and microarray studies, Nucleic Acids Res. 43 (7) (2015) e47.
[38] A. Subramanian, P. Tamayo, V.K. Mootha, S. Mukherjee, B.L. Ebert, M.A. Gillette, et al., Gene set enrichment analysis: a knowledge-based approach for interpreting genome-wide expression profiles, Proc. Natl. Acad. Sci. U. S. A. 102 (43) (2005) 15545–15550.